Multi-component dark matter and Galactic 511 keV gamma-ray emission

Sarif Khan

Chung-Ang University, Seoul

Based on arXiv:2409.07851

Work With: Jinsu Kim, Jongkuk Kim and Pyungwon Ko

Problems in the SM

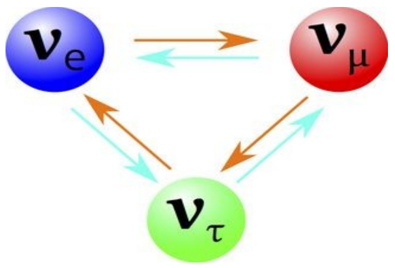

- SM fails to explain neutrino mass and mixing.
- SM doesn't have a DM candidate.
- SM can not explain the observed baryon asymmetry.
- The origin of smallness of the θ-parameter.

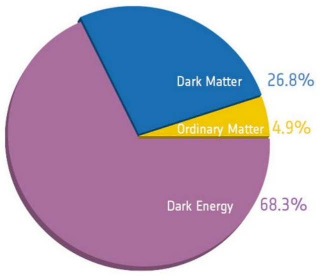

SM Particle Spectrum

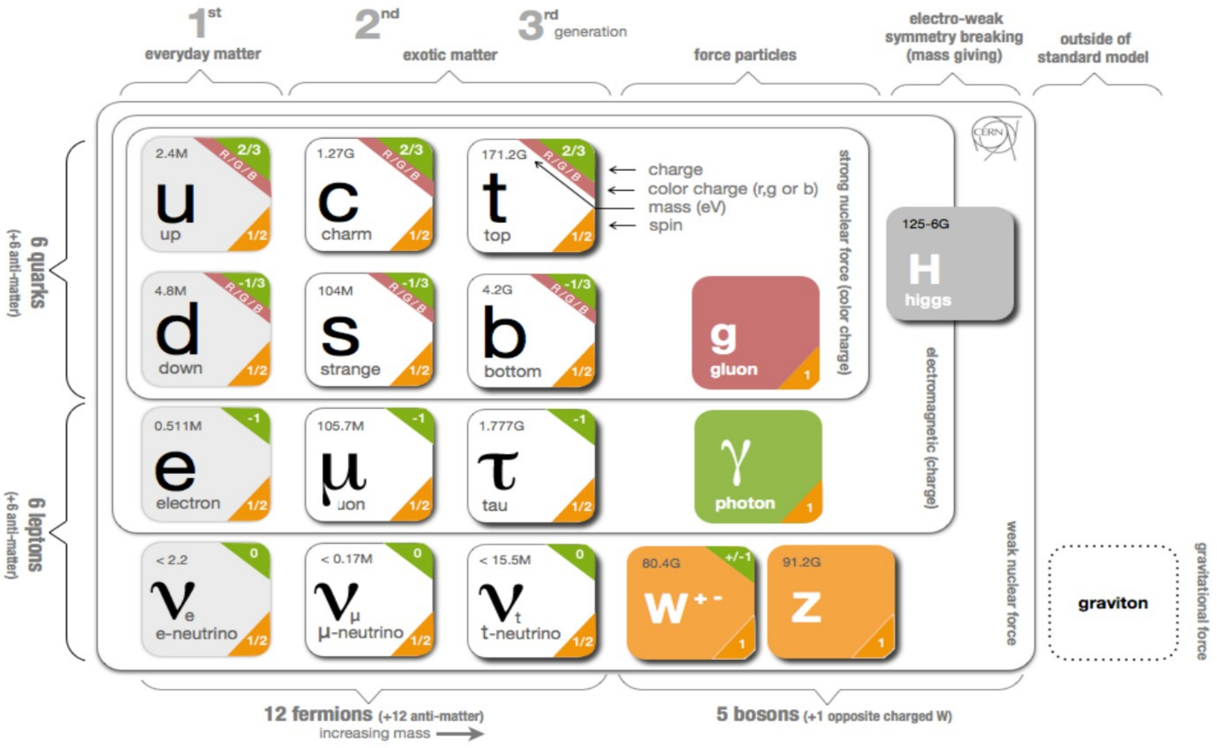

- Neutrino has all the properties mentioned before
- It can not account the whole amount of DM
- Relativistic in nature so no structure formation
- SM is incomplete, need new BSM physics to address DM

Galactic Coordinates

ArXiv:1009.0224, 1012.4515 (PPPC4)

$\bar{J}(\Delta\Omega) = \left(\int_{\Delta\Omega} J\, d\Omega\right)/\Delta\Omega$. The following simple formulæ hold for regions that are disks of aperture $\theta_{\rm max}$ centered around the GC, annuli $\theta_{\rm min} < \theta < \theta_{\rm max}$ centered around the GC or generic regions defined in terms of galactic latitude b and longitude ℓ [23] (provided they are symmetric around the GC):

$$\Delta\Omega = 2\pi \int_0^{\theta_{\rm max}} d\theta\, \sin\theta, \qquad \bar{J} = \frac{2\pi}{\Delta\Omega}\int d\theta\, \sin\theta\, J(\theta), \qquad \text{(disk)}$$

$$\Delta\Omega = 2\pi \int_{\theta_{\rm min}}^{\theta_{\rm max}} d\theta\, \sin\theta, \qquad \bar{J} = \frac{2\pi}{\Delta\Omega}\int d\theta\, \sin\theta\, J(\theta), \qquad \text{(annulus)}$$

$$\Delta\Omega = 4 \int_{b_{\rm min}}^{b_{\rm max}} \int_{\ell_{\rm min}}^{\ell_{\rm max}} db\, d\ell\, \cos b, \qquad \bar{J} = \frac{4}{\Delta\Omega}\iint db\, d\ell\, \cos b\, J(\theta(b,\ell)), \qquad (b\times\ell \text{ region}) \tag{36}$$

where the integration limits in the formulæ for $\bar{J}$ are left implicit for simplicity but obviously correspond to those in $\Delta\Omega$. For the '$b \times \ell$ region' the limits of the integration region are intended to be in one quadrant (e.g. the $b > 0°$, $0 < \ell < 90°$ one for definiteness), hence the factor of 4 to report it to the four quadrants.

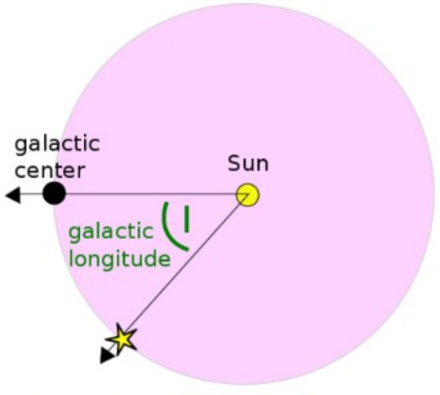

Figure 4: Projection into the galactic plane showing the galactic longitude relative to the Sun.

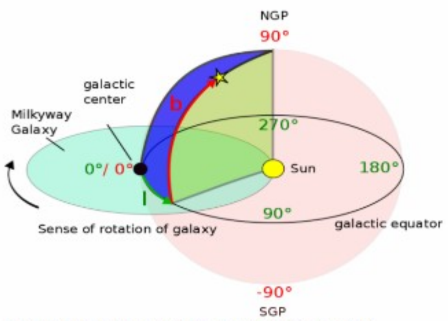

Figure 5: NGP: North Galactic Pole, SGP: South Galactic Pole
l: galactic longitude
b: galactic latitude

$$\rho(r) = \frac{\rho_0[1+(R_0/a)^\alpha]^{(\beta-\gamma)/\alpha}}{(r/R_0)^\gamma[1+(r/a)^\alpha]^{(\beta-\gamma)/\alpha}},$$

↓

$$\text{NFW}: \quad \rho_{\rm NFW}(r) = \rho_s \frac{r_s}{r}\left(1+\frac{r}{r_s}\right)^{-2}$$

↓

DM halo	α	r_s [kpc]	ρ_s [GeV/cm^3]
NFW	–	24.42	0.184

Region	latitude b or aperture θ	longitude l	$\Delta\Omega$ [steradians]	$\bar{J}_{\rm ann}$ NFW	Ein	EinB	Iso	Bur	Moore	$\bar{J}_{\rm dec}$ NFW	Ein	EinB	Iso	Bur	Moore
'GC 0.1°'	$\theta < 0.1°$	–	$0.96\ 10^{-5}$	11579	3579	55665	17.2	6.21	81751	26.3	25.4	55.3	6.45	4.47	44.9
'GC 0.14°'	$\theta < 0.14°$	–	$0.19\ 10^{-4}$	8255	3206	43306	17.2	6.21	52395	25.1	25.0	52.9	6.45	4.47	41.5
'GC 1°'	$\theta < 1°$	–	$0.96\ 10^{-3}$	1118	1196	6945	17.2	6.21	3855	18.0	21.0	35.5	6.45	4.47	24.9
'GC 2°'	$\theta < 2°$	–	0.004	542	711	3103	17.2	6.19	1521	15.5	18.6	28.7	6.45	4.47	20.2
'Gal Ridge'	$0° < \lvert b\rvert < 0.3°$	$0° < \lvert\ell\rvert < 0.8°$	$0.29\ 10^{-3}$	1904	1605	11828	17.2	6.21	7927	19.6	22.2	39.9	6.45	4.47	28.4
'3 × 3'	$0° < \lvert b\rvert < 3°$	$0° < \lvert\ell\rvert < 3°$	0.011	306	443	1577	17.1	6.16	741	13.6	16.4	23.6	6.43	4.46	16.9
'5 × 5'	$0° < \lvert b\rvert < 5°$	$0° < \lvert\ell\rvert < 5°$	0.030	174	264	783	16.8	6.10	367	11.8	14.1	19.0	6.39	4.44	14.0
'5 × 30'	$0° < \lvert b\rvert < 5°$	$0° < \lvert\ell\rvert < 30°$	0.183	47.7	70.5	170	12.1	5.16	84.8	7.27	8.24	9.74	5.55	4.12	7.99
'10 × 10'	$0° < \lvert b\rvert < 10°$	$0° < \lvert\ell\rvert < 10°$	0.121	77.7	118	280	15.5	5.85	138	9.30	10.9	13.4	6.19	4.37	10.5
'10 × 30'	$0° < \lvert b\rvert < 10°$	$0° < \lvert\ell\rvert < 30°$	0.364	35.5	51.8	109	11.7	5.09	57.2	6.86	7.71	8.89	5.48	4.10	7.44
'10 × 60'	$0° < \lvert b\rvert < 10°$	$0° < \lvert\ell\rvert < 60°$	0.727	19.5	27.8	56.7	7.59	3.91	30.4	5.06	5.51	6.13	4.39	3.57	5.36
'GP w/o GC'	$0° < \lvert b\rvert < 5°$	$30° < \lvert\ell\rvert < 180°$	0.913	1.32	1.35	1.38	1.28	1.24	1.33	1.85	1.85	1.86	1.90	1.88	1.85
'sides of GC'	$0° < \lvert b\rvert < 10°$	$10° < \lvert\ell\rvert < 30°$	0.242	14.4	18.5	24.0	9.79	4.70	16.7	5.64	6.12	6.62	5.12	3.96	5.90
'outer Galaxy'	$0° < \lvert b\rvert < 10°$	$90° < \lvert\ell\rvert < 180°$	1.091	0.560	0.535	0.518	0.535	0.671	0.551	1.30	1.29	1.29	1.35	1.39	1.30
'10–20'	$10° < \lvert b\rvert < 20°$	$0° < \lvert\ell\rvert < 180°$	2.116	3.23	3.85	4.62	2.57	1.77	3.58	2.43	2.50	2.58	2.40	2.21	2.47
'20–60'	$20° < \lvert b\rvert < 60°$	$0° < \lvert\ell\rvert < 180°$	6.585	1.64	1.71	1.78	1.57	1.44	1.67	2.05	2.06	2.08	2.10	2.05	2.06
'Gal Poles'	$60° < \lvert b\rvert < 90°$	$0° < \lvert\ell\rvert < 180°$	1.684	0.992	0.965	0.947	0.964	1.11	0.982	1.77	1.75	1.75	1.82	1.88	1.77

Table 2: *Some popular observational regions, their angular area and the corresponding values of the* ***average*** $\bar{J}$ ***factor*** *for different DM halo profiles, in the case of annihilation and decay. 'GP' stands for Galactic Plane and 'GC' for Galactic Center. With a slight abuse of notation we indicate the absolute value of the longitude* $|\ell|$ *to signify that the considered regions are always symmetrical with respect to the* $\ell = 0$ *axis (for instance* $0° < \ell < 3°$ *actually means* $\ell > 357°$, $\ell < 3°$*).*

DM Spike 2410.16379 Luque et al → Explain Signal Morphology better

Early 511 keV line and INTEGRAL

- The 511 keV line is of particular interest, originating from positron annihilation in various astrophysical and cosmological contexts.
- A series of 12 balloon and satellite experiments dating back to 1970 established the existence of a powerful, compact, and variable source of 511 keV positron-annihilation line radiation in the galactic center.
- Following early reports of a line near 511 keV, the first high resolution measurements established its identification as positron annihilation. [**Leventhal et al. 1978**]
- OSSE on the Compton Gamma-Ray Observatory (CGRO) made extensive observations of the 511 keV emission, confirming the nature of the emission as constant, extended along the galactic plane with a strong concentration towards the Galactic centre. [**Purcell et al. 1993, 1997**]
- SPI is the gamma-ray spectrometer aboard INTEGRAL (**launched in 2002 by ESA**), designed to observe high-energy photons in the range of 20 keV to 8 MeV.
- The INTEGRAL sky survey has excellent exposure of the entire inner Galaxy. This led to a first all-sky image of positron annihilation gamma-rays. [**Knödlseder et al. 2003, 2005**]
- INTEGRAL/SPI data accumulated over eleven years and confirmed the detection of the main extended components of characteristic annihilation gamma-ray signatures, altogether at 58σ significance in the 511 keV line. [**Siegert et al. 2016**]

INTEGRAL-SPI

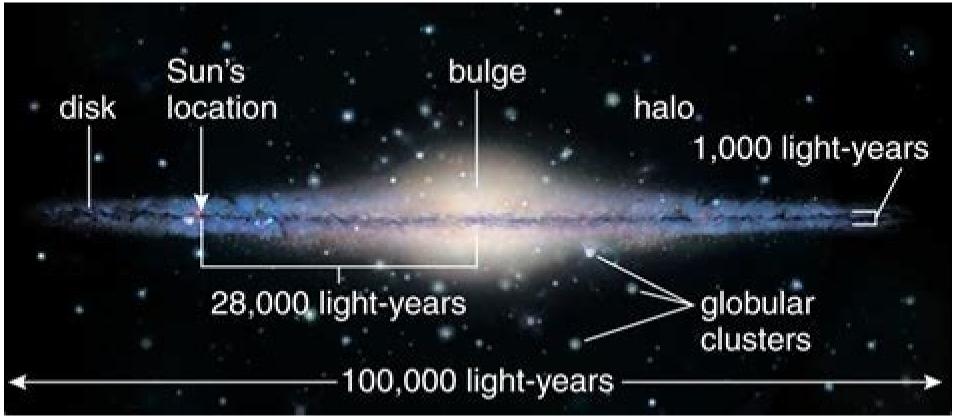

arXiv:1512.00325

Field	Value
Total intensity	$2.74 \pm 0.25 \times 10^{-3}\,\mathrm{cm}^{-1}\mathrm{s}^{-1}$
Bulge intensity	$0.96 \pm 0.07 \times 10^{-3}\,\mathrm{cm}^{-1}\mathrm{s}^{-1}$
Disk intensity	$1.66 \pm 0.35 \times 10^{-3}\,\mathrm{cm}^{-1}\mathrm{s}^{-1}$
Bulge/disk ratio	0.58 ± 0.13
Bulge extent $(\sigma_\ell,\ \sigma_b)$	(8.7, 8.7) [degrees]
Disk extent $(\sigma_\ell,\ \sigma_b)$	$(60^{+10}_{-5}, 10.5^{+2.5}_{-1.5})$ [degrees]
Ps fraction f_{Ps} (bulge)	1.080 ± 0.029
Injection energy of e^+	$\lesssim 3\,\mathrm{MeV}$

$$\frac{d\Phi_{511}}{d\Omega} = 4 \times 10^3 \left(\frac{g_{B-L}}{10^{-20}}\right)^2 \left(\frac{\Delta m}{m_e}\right)^{1/2} \times \tilde{D}_{\mathrm{N}}(\cos\theta)\ [\mathrm{cm}^{-2}\mathrm{s}^{-1}\mathrm{sr}^{-1}]$$

Flux

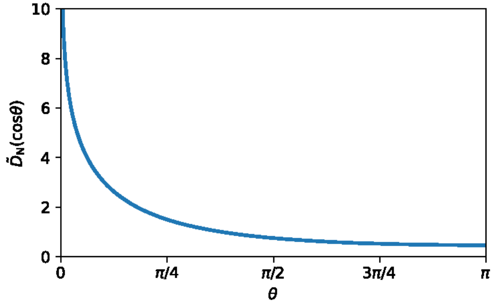

Hayashi et al. 2408.12155 using Threshold effect due to the Sommerfeld effect

Yanagida et al 22

Possible Sources

- Radioactive decay of beta-plus unstable isotopes, such as Ni, Ti, Al, N, produced in nucleosynthesis sources throughout the galaxy.
- Accreting binary system, producing jets loaded with pair plasma, microquasars being the prominent examples.
- Pulsars, because curvature radiation produces and ejects pair plasma.
- The supermassive black hole in our GC (sgr A) through various mechanisms
- DM decay or annihilation, as DM would be gravitationally concentrated in the inner galaxy.
- The Puzzle for the 511 keV line sources still remains and no conclusive candidate has emerged.

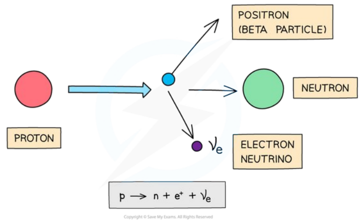

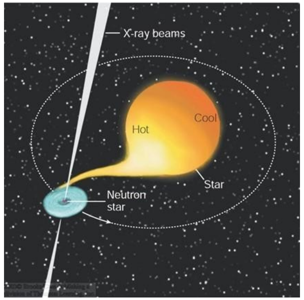

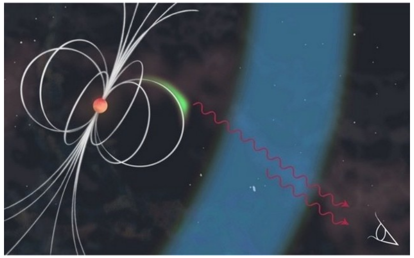

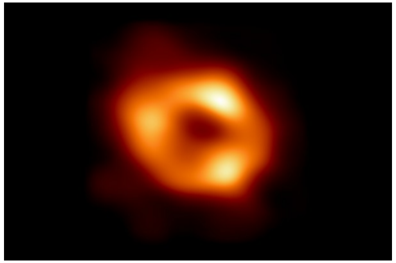

Positron energy below 3 MeV

Beacom et al PRL 06

- 511 keV line can be produced from the electron and positron through Inflight annihilation (IA) and Internal Bremstrahlung (IB).
- As depicted in the top figure, IA can be the potential source 511 keV line if the energy of positron is smaller than 3 MeV and IB is disfavoured because broadening shape in spectra.
- Authors have assumed that rates of positron production, energy loss and annihilation are nearly in equilibrium when average over the propagation timescale (< 3 Myr for < 3 MeV)
- The bottom figure disallows the positron energy above 3 MeV from the diffuse gamma ray spectra (black line) obtained by INTEGRAL and COMPTEL.
- In the present work, we are going to consider e+ e- production below 3 MeV when we explain the 511 keV line

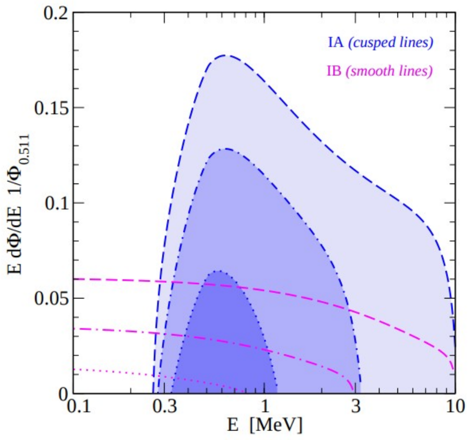

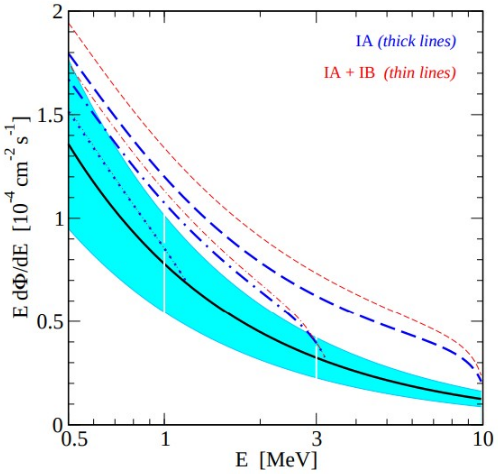

511 KeV line from Positronium

- Positronium is a short lived, exotic atom like system formed by the binding of positron and electron.
- The formation depends on their kinetic energy and the conditions in the medium. If the positronium has lost energy (e.g. scattering), it can capture electron to form positronium.
- The electron and positron eventually annihilate, releasing energy in the form gamma-rays.
- Positronium can be in two states Para-positronium (25%) and Ortho-positronium (75%) depending on the orientation of the spins of electron and positron
- Para-positronium represents total spin zero which can decay to two photons of 511 keV photon energy.
- Ortho-positronium represents total spin equal to one and having three states which decays to three photon of lower energy than electron mass.

Property	Para-Positronium	Ortho-Positronium
Spin	Anti-parallel	Parallel
Photon decay	2 photons (511 keV)	3 photons (low energy)
Lifetime	~ 100 picoseconds	~100 nanoseconds

WIMP, FIMP and SW DM

Hall et al' 09

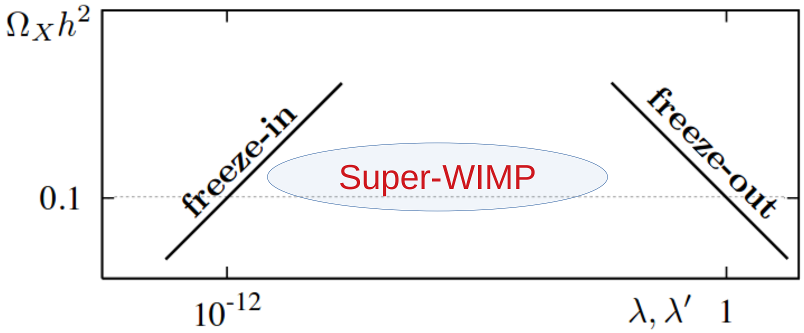

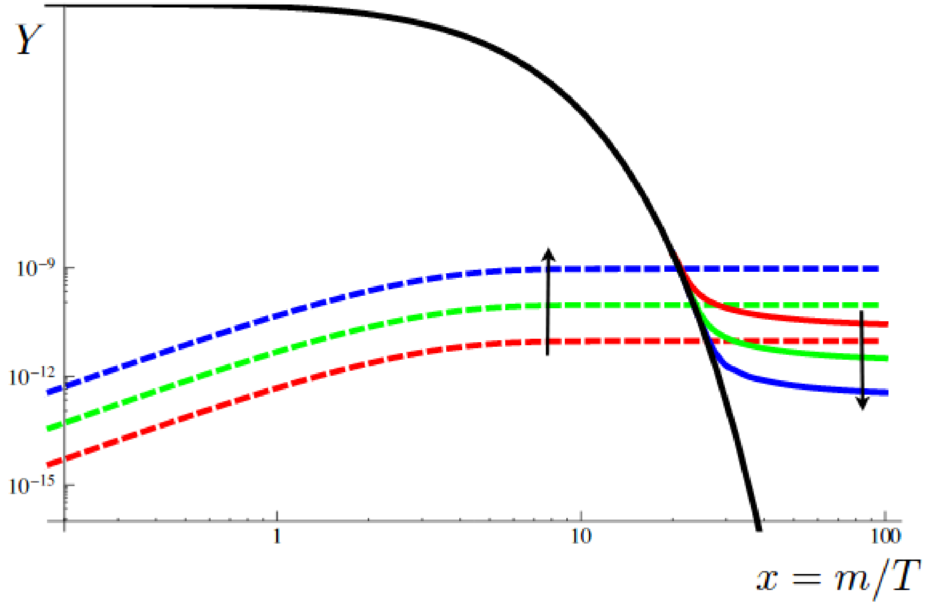

- WIMP DM is easy to detect but no signal puts bound on its parameter space
- FIMP DM is difficult to probe in different experiments due to its feeble interaction
- This work has both WIMP and FIMP type DM depending on choice of U1D charge

- In the present model we have MeV scale WIMP and FIMP
- We can also produce DM from the superWIMP mechanism during the study of FIMP DM.

Minimal Model Construction

- Lagrangian for minimal particle content:

$$\mathcal{L}_{\mathrm{M}} = \mathcal{L}_{\overline{\mathrm{SM}}} - \frac{1}{4}\hat{X}_{\mu\nu}\hat{X}^{\mu\nu} - \frac{\sin\epsilon}{2}\hat{X}_{\mu\nu}\hat{B}^{\mu\nu} + |D\phi_D|^2 + |DH|^2 - V(\phi_D, H)$$

- Potential including both the Higgses:

$$V(\phi_D, H) = -\mu_D^2|\phi_D|^2 + \lambda_D|\phi_D|^4 - \mu_H^2|H|^2 + \lambda_H|H|^4 + \lambda_{HD}|\phi_D|^2|H|^2 .$$

- Relation between mass and flavor gauge basis

Babu et al PRD 98

$$\hat{B}_\mu = \cos\theta_w A_\mu - (\tan\epsilon\sin\zeta + \sin\theta_w\cos\zeta)\, Z_\mu - (\tan\epsilon\cos\zeta - \sin\theta_w\sin\zeta)\, Z_{D\mu} ,$$

$$\hat{X}_\mu = \frac{\sin\zeta}{\cos\epsilon} Z_\mu + \frac{\cos\zeta}{\cos\epsilon} Z_{D\mu} ,$$

$$\hat{W}_\mu^3 = \sin\theta_w A_\mu + \cos\theta_w\cos\zeta Z_\mu - \cos\theta_w\sin\zeta Z_{D\mu} .$$

- Scalars after taking vevs:

$$H = \frac{1}{\sqrt{2}}\begin{pmatrix} 0 \\ v_H + h \end{pmatrix} , \qquad \phi_D = \frac{1}{\sqrt{2}}(v_D + \phi)$$

$$\longrightarrow \quad m_{h\phi}^2 = \begin{pmatrix} 2\lambda_H v_H^2 & \lambda_{HD} v_H v_D \\ \lambda_{HD} v_H v_D & 2\lambda_D v_D^2 \end{pmatrix}$$

$$h_1 = h\cos\theta + \phi\sin\theta ,$$
$$h_2 = \phi\cos\theta - h\sin\theta ,$$

511 keV flux estimate

$$\rho_{\rm DM} = \frac{\rho_s}{r/r_s(1+r/r_s)^2}\,,$$

- Number density of positron:

$$\dot{n}_{e^+} = \frac{1}{m_{Z_D}}\Gamma_{Z_D\to e^-e^+}\rho_{\rm DM} + \frac{1}{2m_{Z_D}^2}\langle\sigma v\rangle_{Z_DZ_D\to e^-e^+}\rho_{\rm DM}^2\,,$$

- Photon flux from the annihilation of positronium: $\frac{d\Phi_\gamma^{511}}{d\Omega} = \frac{1}{4\pi}\int_{\rm l.o.s.}\dot{n}_\gamma\, ds\,.$

$$\begin{aligned}\frac{d\Phi_\gamma^{511}}{d\Omega} &= \frac{\Gamma_{Z_D\to e^-e^+}}{8\pi m_{Z_D}}\int_{\rm l.o.s.}\rho_{\rm DM}\,ds + \frac{\langle\sigma v\rangle_{Z_DZ_D\to e^-e^+}}{16\pi m_{Z_D}^2}\int_{\rm l.o.s.}\rho_{\rm DM}^2\,ds \\ &= \frac{\Gamma_{Z_D\to e^-e^+}}{8\pi m_{Z_D}}R_\odot\rho_\odot J_{\rm decay}(\psi) + \frac{\langle\sigma v\rangle_{Z_DZ_D\to e^-e^+}}{16\pi m_{Z_D}^2}R_\odot\rho_\odot^2 J_{\rm ann}(\psi)\,,\end{aligned}$$

where

$$J_{\rm decay} \equiv \int_{\rm l.o.s.}\frac{\rho_{\rm DM}}{\rho_\odot}\frac{ds}{R_\odot}\,, \qquad J_{\rm ann} \equiv \int_{\rm l.o.s.}\left(\frac{\rho_{\rm DM}}{\rho_\odot}\right)^2\frac{ds}{R_\odot}\,,$$

- Total flux after integrating along bulge:

$$\Phi_\gamma^{511} = \int_{\psi<10.275^\circ} \frac{d\Phi_\gamma^{511}}{d\Omega}\, d\Omega\,.$$

We note that

$$\int_{\psi<10.275^\circ} J_{\rm decay}\, d\Omega \approx 1.2\,, \qquad \int_{\psi<10.275^\circ} J_{\rm ann}\, d\Omega \approx 9.7\,.$$

$$\langle\sigma v\rangle_{Z_D Z_D\to e^-e^+} \approx \frac{\cos^2\theta\sin^2\theta y_e^2 v_D^2 g_D^4 (m_{h_1}^2 - m_{h_2}^2)^2}{12\pi(m_{h_1}^2 - 4m_{Z_D}^2)^2(m_{h_2}^2 - 4m_{Z_D}^2)^2}\left(1 - \frac{m_e^2}{m_{Z_D}^2}\right)^{3/2},$$

Annihilation cross section

$$\Gamma_{Z_D\to e^-e^+} = \frac{m_{Z_D} e^2\cos^2\zeta}{12\pi\cos^2\theta_w\sin^2\theta_w}\sqrt{1-\frac{4m_e^2}{m_{Z_D}^2}} \times\left[V_{Z_De^-e^+}^2 + A_{Z_De^-e^+}^2 + \frac{2m_e^2}{m_{Z_D}^2}\left(V_{Z_De^-e^+}^2 - 2A_{Z_De^-e^+}^2\right)\right],$$

Decay Width

$$\langle\sigma v\rangle_{Z_D Z_D\to e^-e^+} \simeq \left(\frac{m_{Z_D}}{\rm MeV}\right)^2 \times 10^{-30}\ {\rm cm}^3/{\rm s}\,,$$

Required CS for 511 keV but conflict DM density

$$\tau_{Z_D} \simeq \left(\frac{\rm MeV}{m_{Z_D}}\right)\times 8\times 10^{26}\ {\rm s}\,.$$

Required Decay for 511 but need total DM density???

Multi-Component Scenarios $\rightarrow$ $\boxed{n_{\psi_D} \neq 1/2}$

Complete Lagrangian for multi component DM:

$$\mathcal{L}_{n_{\psi_D} \neq 1/2} = \mathcal{L}_{\mathrm{M}} + \bar{\psi}_D \left(i\gamma^\mu D_\mu - m_{\psi_D} \right) \psi_D$$

$$D_\mu \psi_D = \partial_\mu \psi_D - i g_D n_{\psi_D} \hat{X}_\mu \psi_D$$

Evolution of both the DM:

$$\frac{dY_i}{dx_i} = -\frac{s(x_i)\langle\sigma v\rangle_i}{x_i H(x_i)} \left[Y_i^2 - (Y_i^{\mathrm{eq}})^2 \right], \qquad i = \{Z_D, \psi_D\},$$

$$s(x_i) = \frac{2\pi^2}{45} g_{*,s} m_i^3 x_i^{-3}, \quad H(x_i) = \sqrt{\frac{g_* \pi^2}{90}} \frac{m_i^2}{M_{\mathrm{P}}} x_i^{-2},$$

DM Relic density analytical estimate and 511 keV

$$n_i^{\rm eq}\langle\sigma v\rangle_i \simeq H(x_i) \text{ at } x_i = x_i^f\,,$$

The BE can be solved analytically from the freeze-out point:

$$Y_i^0 = Y_i^f\left[1+\frac{2\pi^2}{45}\sqrt{\frac{90}{\pi^2}}M_{\rm P}m_iY_i^f\,\frac{g_{*,s}(x_i^f)}{\sqrt{g_*(x_i^f)}}\,\frac{a_i+3b_i/x_i^f}{x_i^f}\right]^{-1},$$

Our Analytical result matches with the publicly available Boltzmann Solver micromega result

$$Y_i^f = \frac{45}{2\pi^4}\sqrt{\frac{\pi}{8}}\frac{g_i}{g_{*,s}(x_i^f)}(x_i^f)^{3/2}e^{-x_i^f}\,.$$

$$a_{Z_D} = \frac{11g_D^4\sqrt{1-r_1}}{288\pi m_{Z_D}^2}\left[\frac{1-\frac{20}{11}r_1+\frac{15}{11}r_1^2-\frac{5}{11}r_1^3+\frac{1}{16}r_1^4}{(1-\frac{3}{4}r_1+\frac{1}{8}r_1^2)^2}\right],$$

$$b_{Z_D} = \frac{13g_D^4r_1\sqrt{1-r_1}}{1728\pi m_{Z_D}^2}\left[\frac{1-\frac{19}{13}r_1+\frac{22}{13}r_1^2-\frac{17}{13}r_1^3+\frac{127}{208}r_1^4-\frac{17}{104}r_1^5+\frac{1}{52}r_1^6}{(1-\frac{1}{2}r_1)^4(1-\frac{1}{4}r_1)^3}\right],$$

$$a_{\psi_D} = \frac{g_D^4n_{\psi_D}^4\cos^4\zeta(1-r_2)^{3/2}}{16\pi m_{\psi_D}^2\cos^4\epsilon\left(1-\frac{1}{2}r_2\right)^2},$$

$$b_{\psi_D} = \frac{g_D^4n_{\psi_D}^4\cos^4\zeta\sqrt{1-r_2}}{8\pi m_{\psi_D}^2\cos^4\epsilon}\left[\frac{1-\frac{2}{3}r_2+\frac{1}{8}r_2^2+\frac{1}{6}r_2^3}{\left(1-\frac{1}{2}r_2\right)^4}\right],$$

RD for two DM components

$$\Omega_{\rm DM}h^2 = \Omega_{Z_D}h^2+\Omega_{\psi_D}h^2 = \frac{s_0h^2}{\rho_{\rm crit}}\left(m_{Z_D}Y_{Z_D}^0+m_{\psi_D}Y_{\psi_D}^0\right),$$

$$\frac{d\Phi_\gamma^{511}}{d\Omega} = f_{Z_D}\frac{\Gamma_{Z_D\to e^-e^+}}{8\pi m_{Z_D}}R_\odot\rho_\odot J_{\rm decay}(\psi)+f_{Z_D}^2\frac{\langle\sigma v\rangle_{Z_DZ_D\to e^-e^+}}{16\pi m_{Z_D}^2}R_\odot\rho_\odot^2J_{\rm ann}(\psi)\,,$$

511 keV flux

DM bounds for WIMP case

- DM relic density bound put by Planck 2018 data
- Invisible Higgs decay and BSM Higgs bound
- Direct detection bound
- Indirect detection and 511 keV line
- N_eff bound
- CMB bound

Range of model parameters for scatter plots

$$1 \le m_{Z_D}\,[\mathrm{MeV}] \le 100\,, \quad 1 \le m_{h_2}\,[\mathrm{MeV}] \le 100\,,$$
$$10^{-5} \le \theta \le 0.1\,, \quad 10^{-2} \le g_D \le \sqrt{4\pi}\,, \quad 10^{-25} \le \epsilon, \zeta \le 10^{-17}\,,$$
$$1 \le m_{\psi_D}\,[\mathrm{GeV}] \le 100\,, \quad 10^{-2} \le n_{\psi_D} g_D \le \sqrt{4\pi}\,.$$

Scatter plot 1

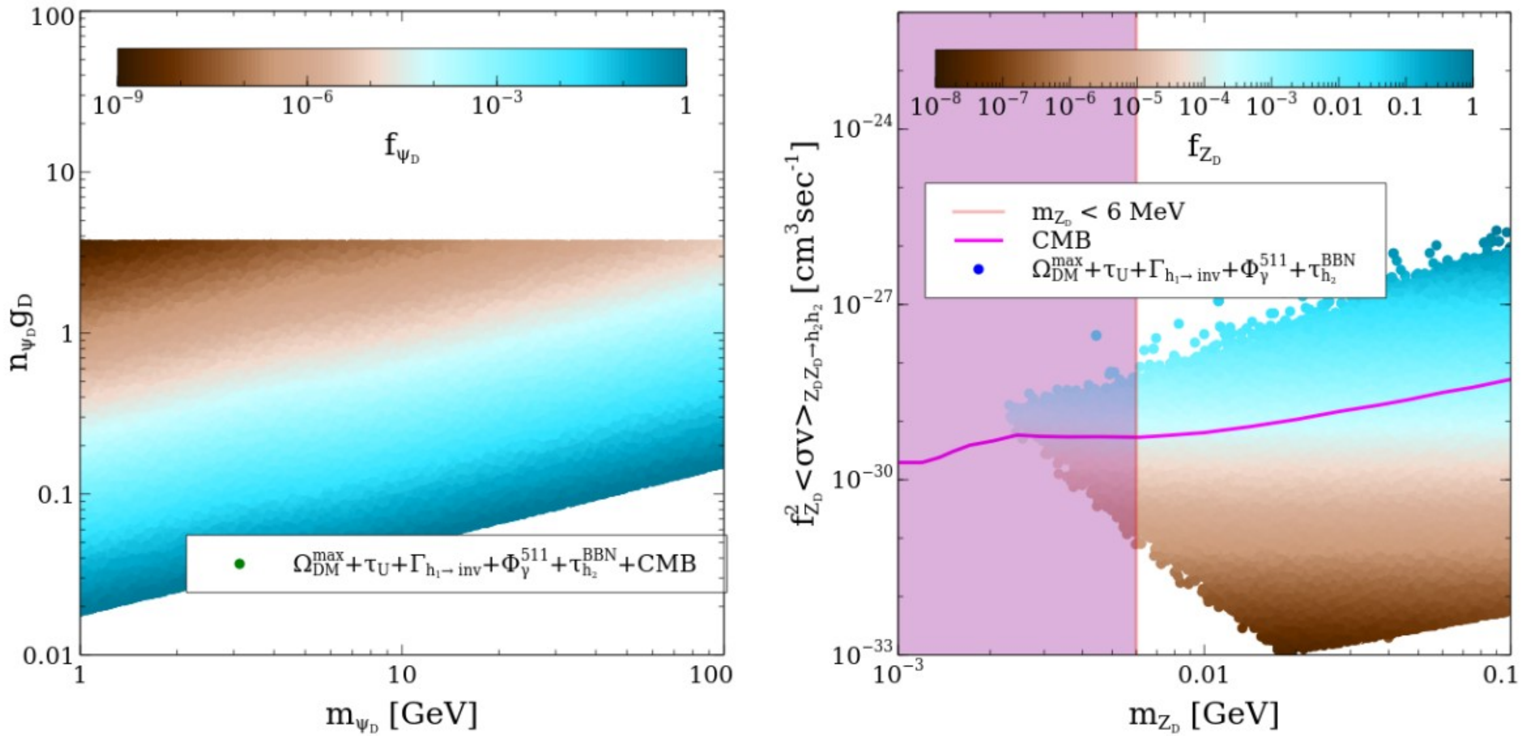

- The general behaviour from the LP indicates that if we increase n_psi g_D, then the DM relic density will decrease, and if we increase the m_{\psi_D}, then the psi_D relic density will increase as the comoving number density effectively varies as

Scatter plot 2

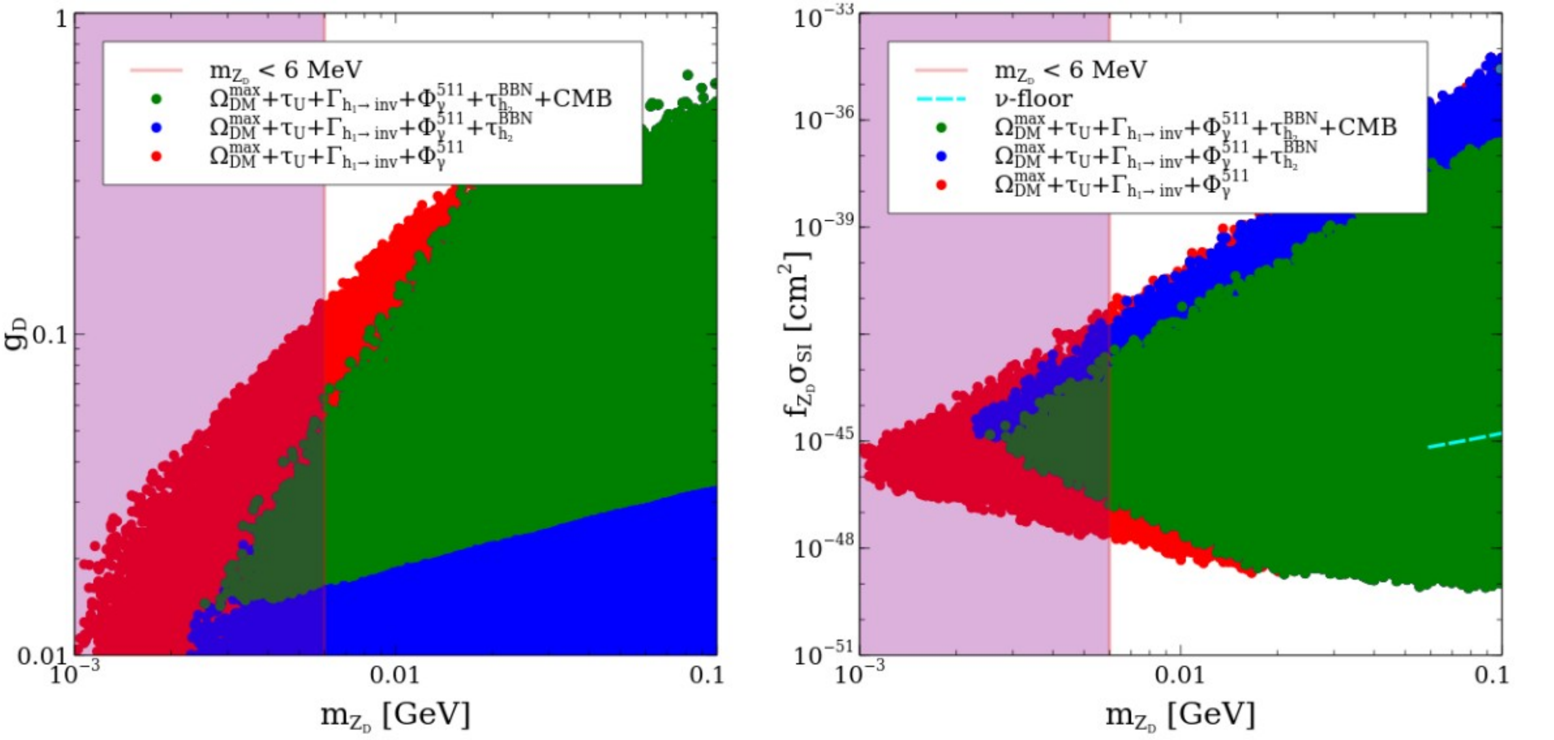

- The LP and RP show the allowed parameter space in the m_ZD-g_D and m_ZD-f_ZD sigma_SI planes.
- The colour variation in both plots implies the application of successive bounds.

Scatter plot 3

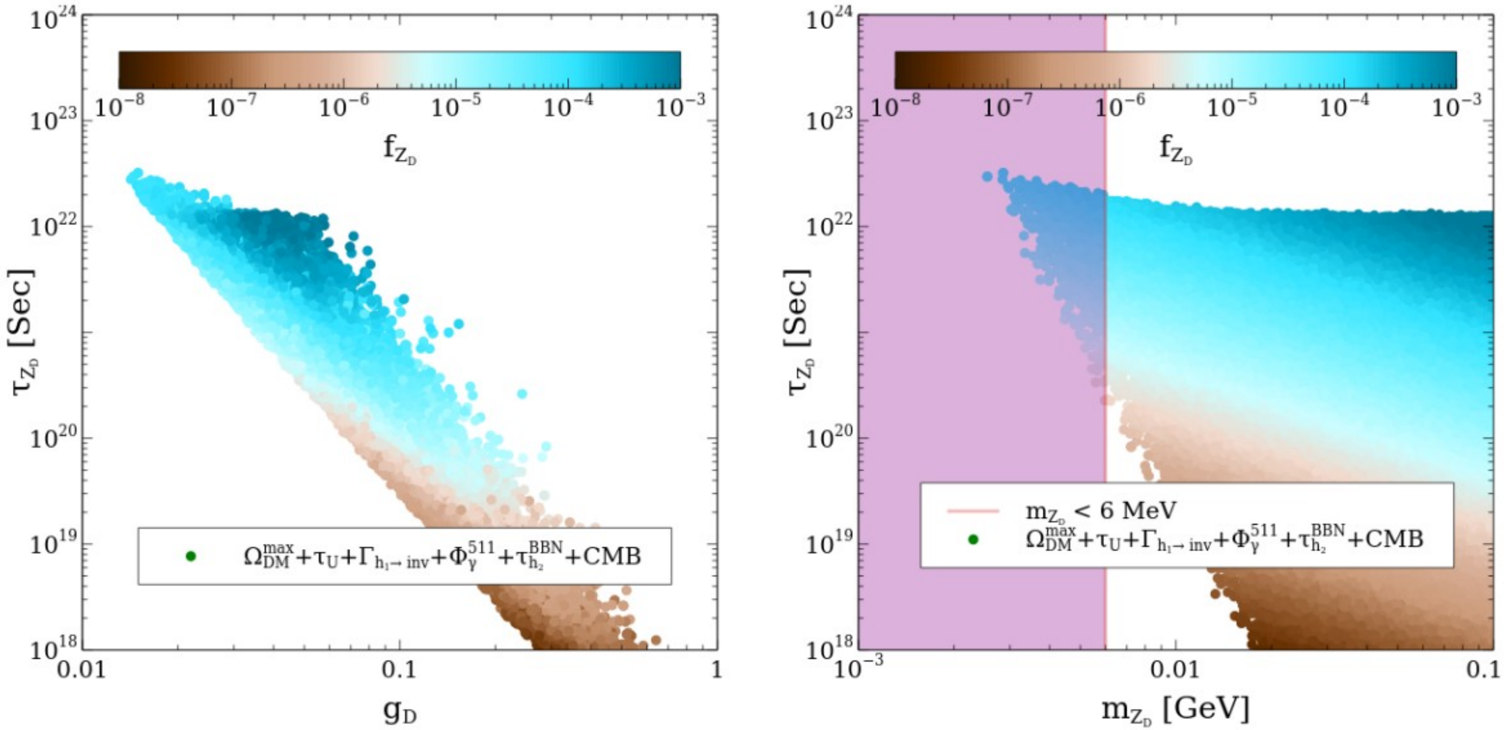

- The Z_D DM lifetime as a function of g_D (left) and m_ZD (right)
- Flux is proportional to f_ZD/tau_ZD, so anti-correlation in LP
- We also observe that tau_ZD becomes comparable to the age of the Universe when f_ZD ~ 10^-8 – 10^-7.

FIMP DM → $n_\psi = 1/2$

Weinberg PRL 13, Ahmed et al EPJC18

- The Lagrangian in the present case

$$\mathcal{L}_{1/2} = \mathcal{L}_{\mathrm{M}} + \bar{\psi}_D \left(i\gamma^\mu D_\mu - m_{\psi_D}\right)\psi_D - \frac{1}{\sqrt{2}}\left(y_{\psi_D}\phi_D^\dagger \overline{\psi_D^C}\psi_D + \mathrm{h.c.}\right) ,$$

- Majorana particle definition

$$\psi_D = \frac{1}{\sqrt{2}}\left(\psi_D^R + i\psi_D^I\right) .$$

Majorana mass

$$m_{\psi_D^{R,I}} = m_{\psi_D} \pm y_{\psi_D} v_D .$$

- Lagrangian in Majorana basis: →

$$\mathcal{L}_{\mathrm{DF}} = \frac{i}{2}\left(\bar{\psi}_+\gamma^\mu\partial_\mu\psi_+ + \bar{\psi}_-\gamma^\mu\partial_\mu\psi_-\right) - \frac{1}{2}m_+\bar{\psi}_+\psi_+ - \frac{1}{2}m_-\bar{\psi}_-\psi_- - \frac{i}{4}g_{\mathrm{X}}\left(\bar{\psi}_+\gamma^\mu\psi_- - \bar{\psi}_-\gamma^\mu\psi_+\right)X_\mu - \frac{y_{\mathrm{X}}}{2}\left(\bar{\psi}_+\psi_+ - \bar{\psi}_-\psi_-\right)\phi .$$

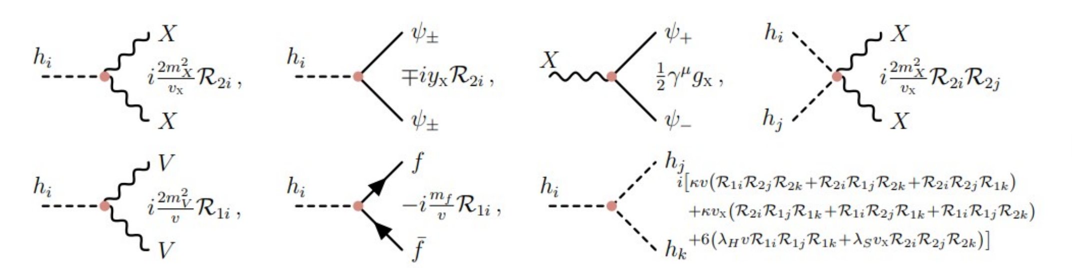

→ Relevant Vertex factors

Boltzmann Eq. For FIMP DM

The complete BE:

$$\frac{dY_{Z_D}}{dz} = \frac{M_{\rm P}\, z\sqrt{g_{\rm eff}(z)}}{0.33 m_{h_1}^2 g_{*,s}(z)}\Bigg[2\sum_{i=1,2}\langle\Gamma_{h_i\to Z_D Z_D}\rangle\left(Y_{h_i}^{\rm eq} - Y_{Z_D}^2\right)\theta(m_{h_i} - 2m_{Z_D})$$

$$+ \langle\Gamma_{\psi_D^R\to\psi_D^I Z_D}\rangle_{\rm NTH}\left(Y_{\psi_D^R} - Y_{\psi_D^I}Y_{Z_D}\right)\theta(m_{\psi_D^R} - m_{\psi_D^I} - m_{Z_D})\Bigg],$$

$$\frac{dY_{\psi_D^{R(I)}}}{dz} = \frac{M_{\rm P}\, z\sqrt{g_{\rm eff}(z)}}{0.33 m_{h_1}^2 g_{*,s}(z)}\Bigg[2\sum_{i=1,2}\langle\Gamma_{h_i\to\psi_D^{R(I)}\psi_D^{R(I)}}\rangle\left(Y_{h_i}^{\rm eq} - Y_{\psi_D^{R(I)}}^2\right)\theta(m_{h_i} - 2m_{\psi_D^{R(I)}})$$

$$-(+)\langle\Gamma_{\psi_D^R\to\psi_D^I Z_D}\rangle_{\rm NTH}\left(Y_{\psi_D^R} - Y_{\psi_D^I}Y_{Z_D}\right)\theta(m_{\psi_D^R} - m_{\psi_D^I} - m_{Z_D})\Bigg], \qquad (3.17$$

Thermal and non-thermal decay width:

$$\langle\Gamma_{h_i\to AA}\rangle = \Gamma_{h_i\to AA}\frac{K_1(z)}{K_2(z)}, \quad \langle\Gamma_{\psi_D^R\to\psi_D^I Z_D}\rangle_{\rm NTH} = m_{\psi_D^R}\Gamma_{\psi_D^R\to\psi_D^I Z_D}\frac{\int\frac{\tilde{f}_{\psi_D^R}d^3p}{\sqrt{p^2+m_{\psi_D^R}}}}{\int\tilde{f}_{\psi_D^R}d^3p},$$

FIMP DM density

$$\Omega_{\rm DM}h^2 = \Omega_{Z_D}h^2 + \Omega_{\psi_D^I}h^2 = \sum_{i=Z_D,\psi_D^I} 2.755\times10^8 Y_i\left(\frac{m_i}{\rm GeV}\right).$$

Analytical estimate for FIMP

DM total density

$$\Omega_{Z_D/\psi^I_D} h^2 = \Omega^{\rm FI}_{Z_D/\psi^I_D} h^2 + \Omega^{\rm SW}_{Z_D/\psi^I_D} h^2 \,,$$

$$\Omega^{\rm FI}_C h^2 = \frac{1.09 \times 10^{27}}{g_{*,s}\sqrt{g_*}} \frac{m_C \Gamma_{A\to BC}}{m_A^2} \,, \qquad \Omega^{\rm SW}_C h^2 = \frac{m_C}{m_A} \Omega^{\rm FI}_A h^2 \,.$$

After using all the expressions

$$\Omega_{Z_D} h^2 \approx 1.08 \times 10^{22} \times \sum_{i=1,2} c_i \frac{m_{Z_D}}{m_{h_i} v_D^2} \Bigg[(\Delta m_{\psi_D})^2 \left(1 - \frac{4 m^2_{\psi^R_D}}{m^2_{h_i}}\right)^{3/2} \theta\left(m_{h_i} - 2 m_{\psi^R_D}\right)$$
$$+ 2 m^2_{h_i} \sqrt{1 - \frac{4 m^2_{Z_D}}{m^2_{h_i}}} \left(1 - \frac{4 m^2_{Z_D}}{m^2_{h_i}} + \frac{12 m^4_{Z_D}}{m^4_{h_i}}\right) \theta\left(m_{h_i} - 2 m_{Z_D}\right) \Bigg] \,, \qquad (3.23)$$

and

$$\Omega_{\psi^I_D} h^2 \approx 1.08 \times 10^{22} \times \sum_{i=1,2} c_i \frac{m_{\psi^I_D} (\Delta m_{\psi_D})^2}{m_{h_i} v_D^2} \Bigg[\left(1 - \frac{4 m^2_{\psi^R_D}}{m^2_{h_i}}\right)^{3/2} \theta\left(m_{h_i} - 2 m_{\psi^R_D}\right)$$
$$+ \left(1 - \frac{4 m^2_{\psi^I_D}}{m^2_{h_i}}\right)^{3/2} \theta\left(m_{h_i} - 2 m_{\psi^I_D}\right) \Bigg] \,, \qquad (3.24)$$

$$\boxed{v_D \propto \frac{M_{Z_D}}{g_D}}$$

Line Plot 1

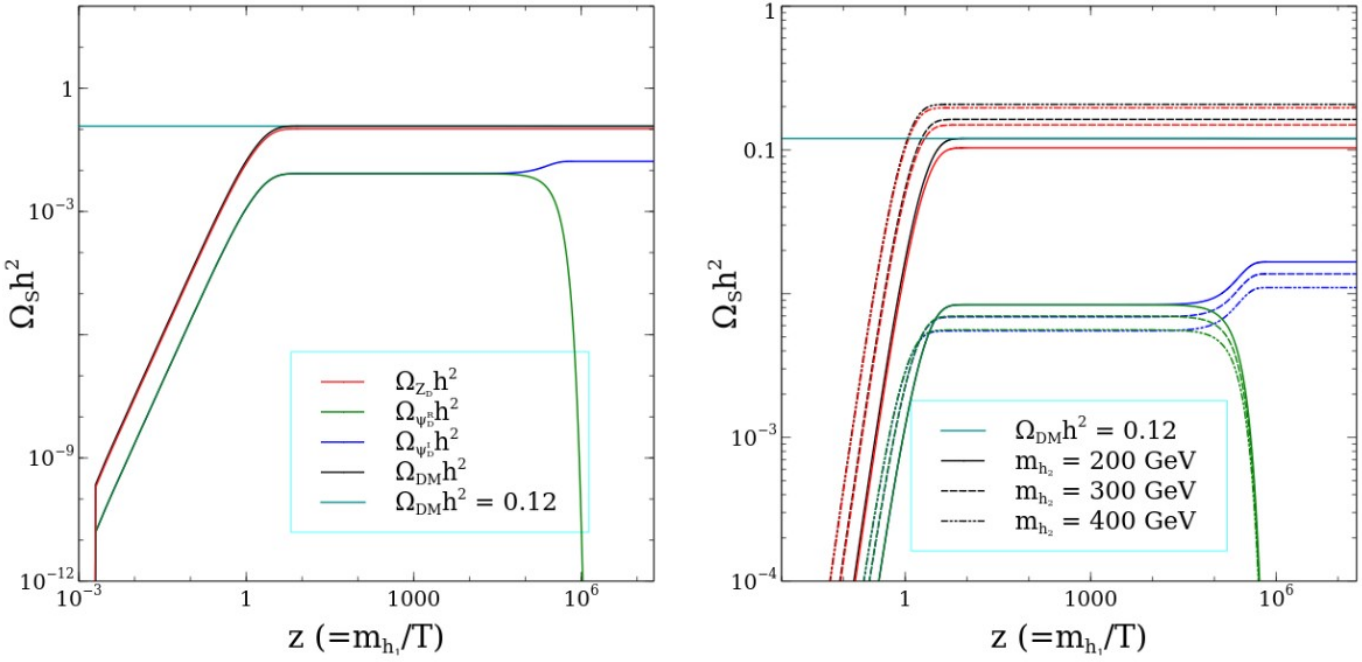

- LP shows the DM RD variation with z produced by different mechanisms.
- RP shows the variation for three different values of BSM Higgs mass.

Line Plot 2

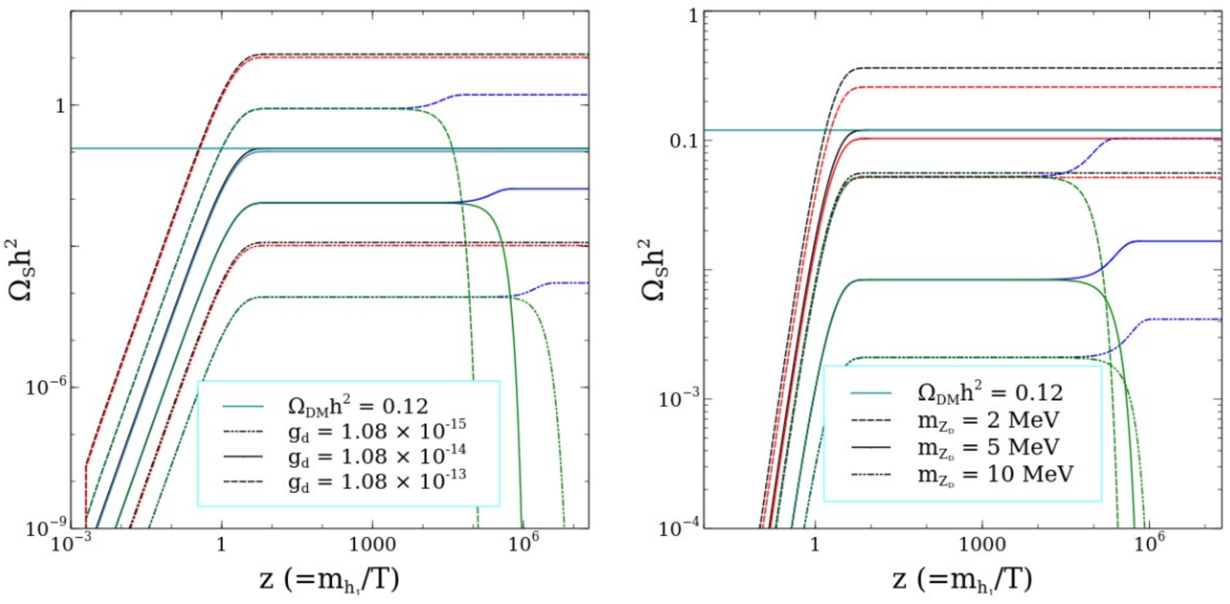

- LP and RP show the DM RD variations for three different values of g_D and m_ZD.
- In both the plots, we see DM RD vary linearly with g_D and inversely with m_ZD as shown by the analytical estimates.

Scatter Plot 1

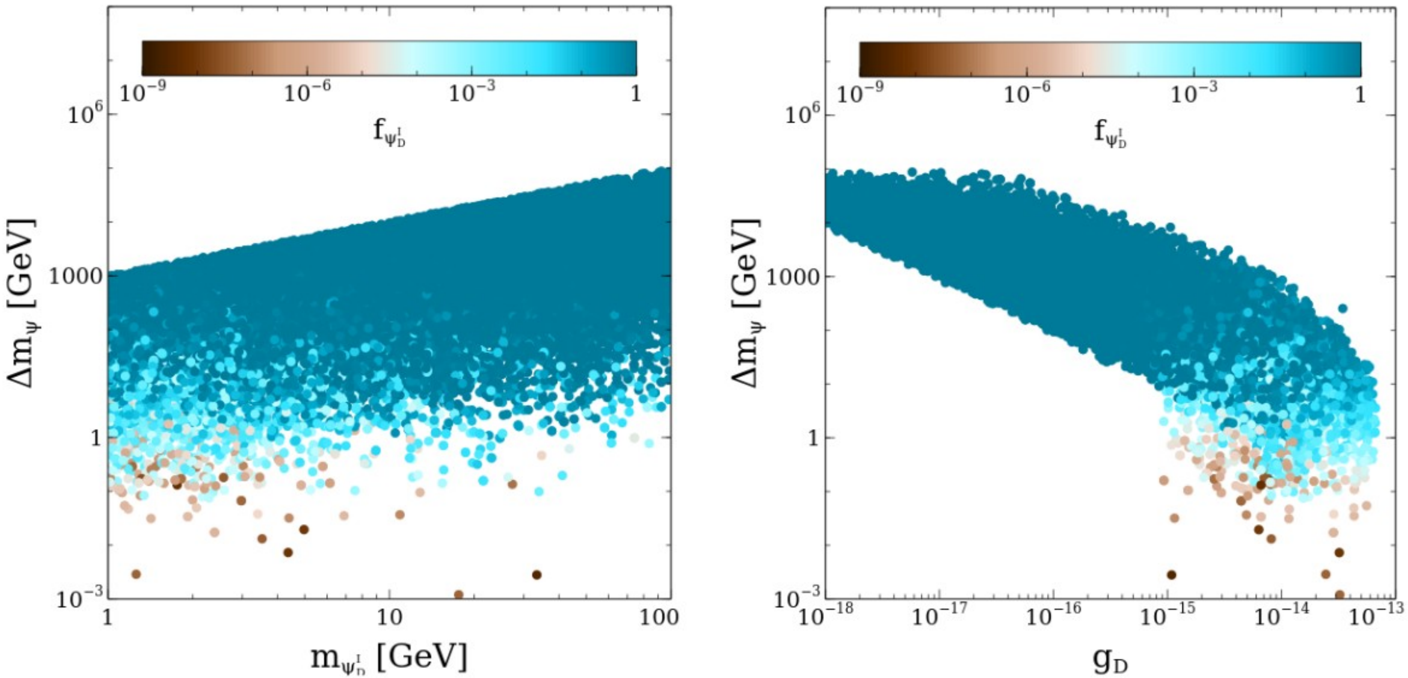

- Left panel shows that f_psi-I increases as the value of Δm_psi increases.
- The right panel indicates that, for g_D < 10^-15, DM is mostly dominated the fermion DM and this region corresponds to Δm > 10 GeV.

Scatter Plot 2

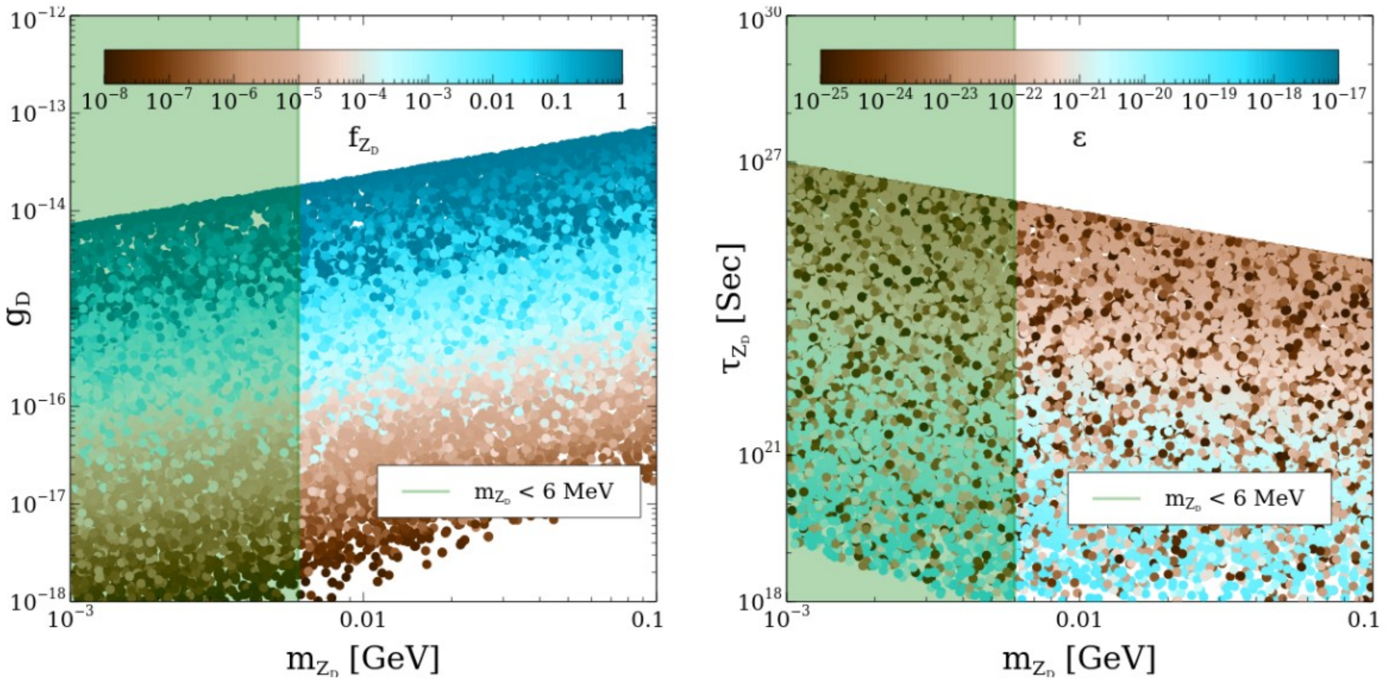

- LP infers that vector DM RD vary with the square of the gauge coupling g_D as shown in the analytical estimates.
- Any fraction of Z_D DM is allowed for the FIMP case to explain the 511 keV line which was not possible for WIMP case.

Scatter Plot 3

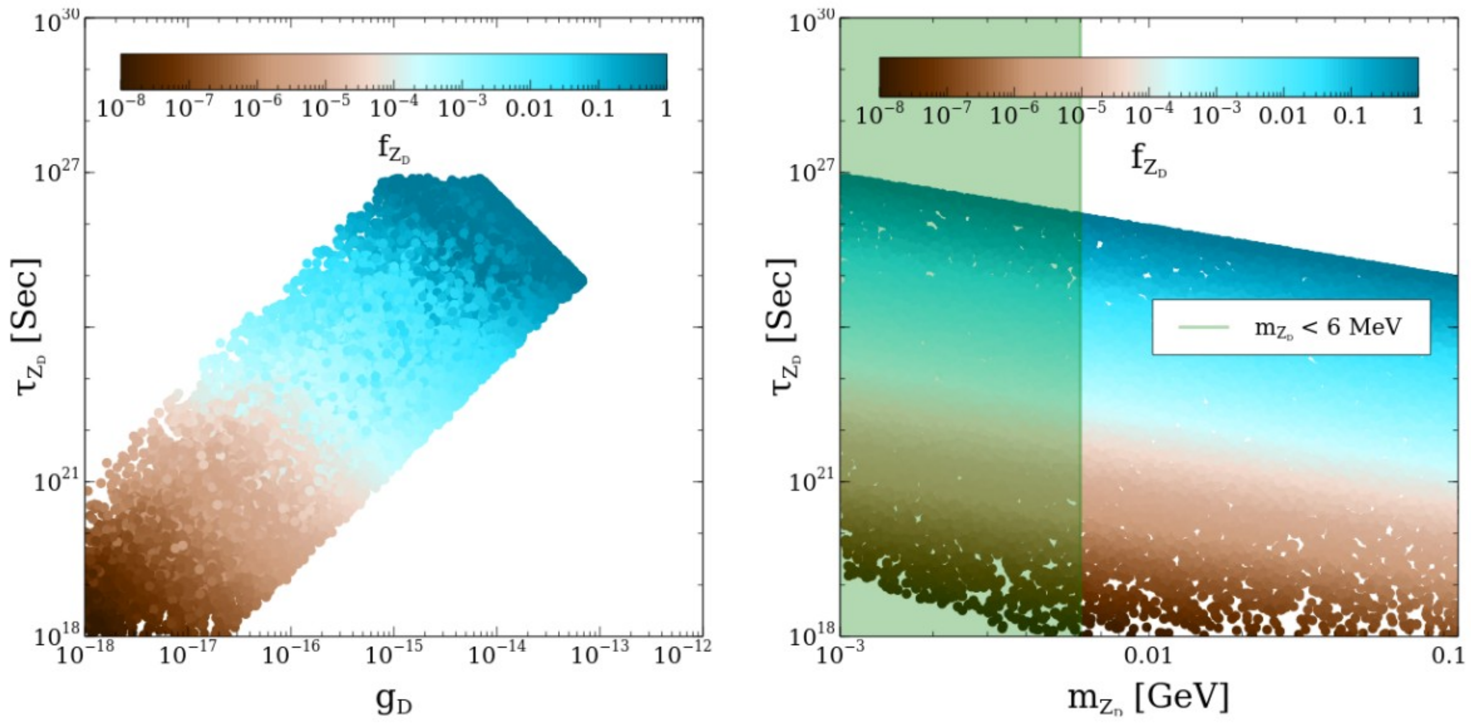

- LP and RP show the lifetime as a function of the gauge coupling g_D and the vector DM mass m_ZD.
- It is clear that the Z_D lifetime is proportional to the fraction of the vector DM relic f_ZD.

N_eff determination

Decant et al JCAP22

Approximate expression of N_eff

$$\Delta N_{\rm eff} = 1.2\times10^{-2}\,\delta_{Z_D}\left(\frac{m_{\psi_D^R}}{100\,{\rm GeV}}\right)\left(\frac{10^{-22}\,{\rm GeV}}{\Gamma_{\psi_D^R\to\psi_D^I Z_D}}\right)^{1/2}\left(\frac{\Omega_{Z_D}h^2}{0.12}\right)\left(\frac{1\,{\rm MeV}}{m_{Z_D}}\right),$$

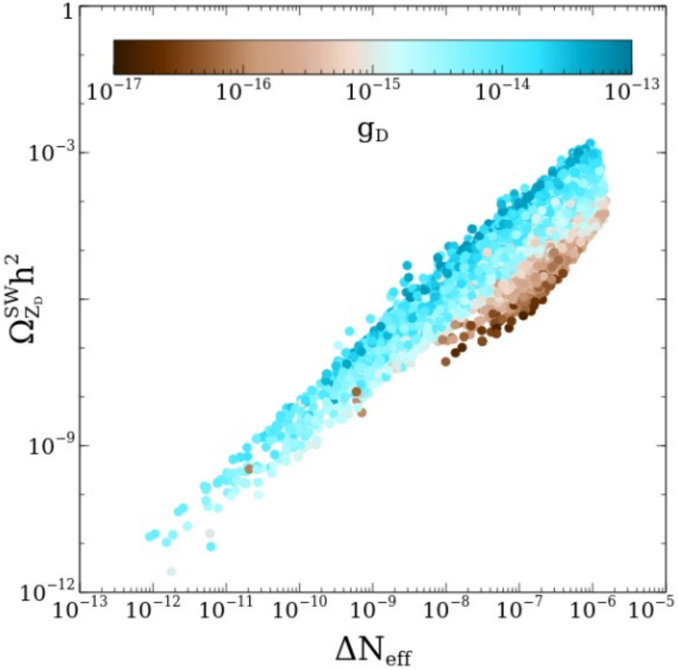

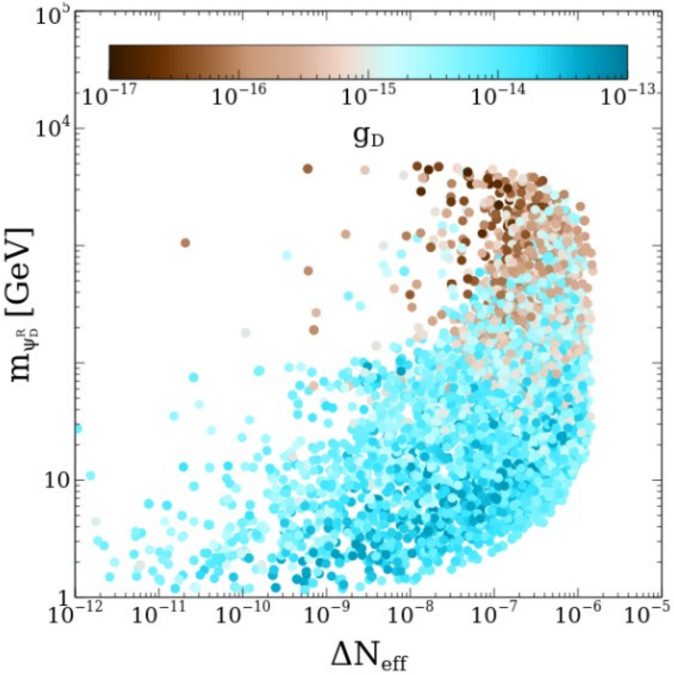

- Due to the suppressed SW contribution N_eff contribution is small and beyond the reach of the CMB-S4.

Conclusion

- The dark U1D naturally accommodates a gauge boson which may decay and/or pair annihilate to the electron-positron pairs due to the presence of the gauge kinetic mixing and the dark Higgs boson.
- Depending on the U1D charge of the dark fermion, one may categorise the model into two; one where the charge is not equal to 1/2 and the other where the charge is 1/2, in which case a Yukawa interaction term can be admitted.
- For the WIMP scenario, we have demonstrated that the case where the vector dark matter becomes the 100% of the total dark matter, which thus corresponds to the minimal scenario, is incapable of explaining both the correct relic density and the 511 keV signal mainly due to the stringent CMB bound. We found f_ZD < 1e-3 from CMB.
- For the FIMP scenario, on the other hand, the fraction of the vector dark matter could become unity, while satisfying all the relevant constraints.
- For WIMP case, the freeze-out of the light vector dark matter may occur during the BBN time in which case the BBN prediction can potentially be altered. Needs separate study.
- For the FIMP case, the lifetime of the vector dark matter may become comparable to the age of the Universe. Thus, it may leave imprints on large scale structures, and future Galaxy-scale surveys can further provide a potential probe.

Thank you for your attention

Back up Slides